New nonlocal approaches for modelling the electrophysiology of the human heart

Newport, June, 2013

Kevin Burrage, (Oxford and QUT)
kevin.burrage@cs.ox.ac.uk

Overview

- Modelling spatial heterogeneity in cardiac electrophysiology and the bidomain equation.
- Coping with tissue heterogeneities – non-local models.
- Validation against experimental and clinical data.
- Discussion on modelling: homogneisation, phenomenological models, intuitive versus non-intuitive models, what do we mean by validation?

Coping with spatial heterogeneity when modelling the electrophysiology of the heart

Structural heterogeneity of cardiac tissue

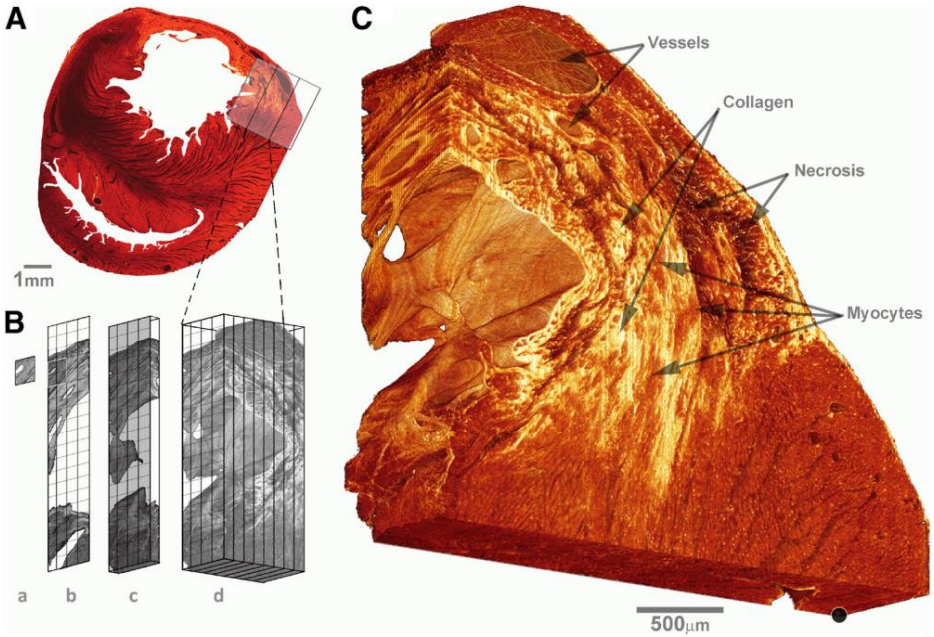

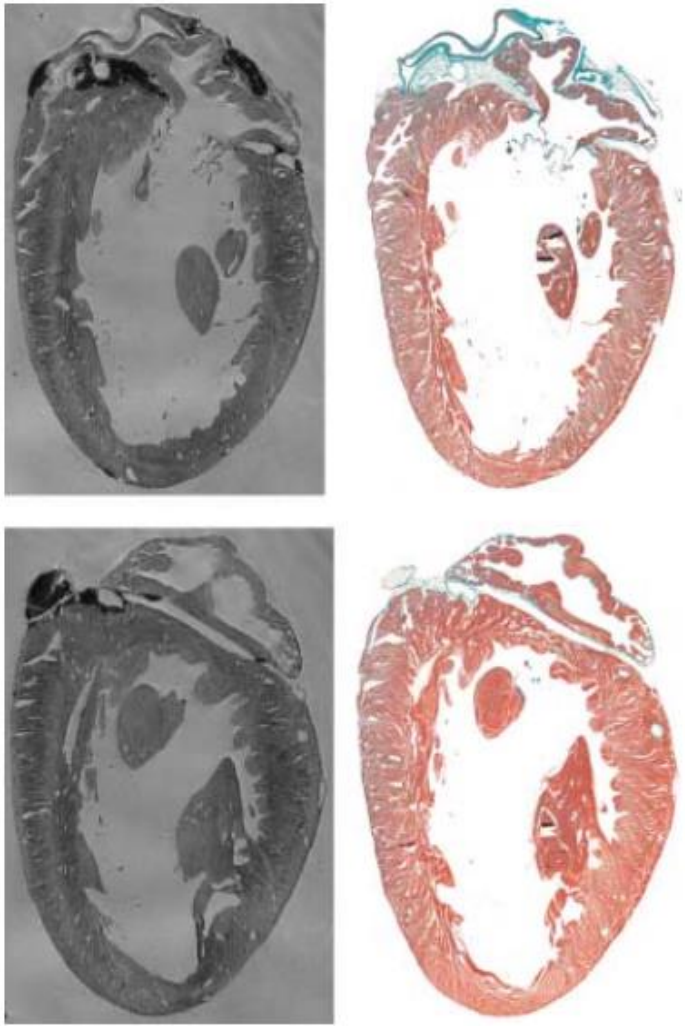

Composition of the extracellular space[1]:

- Ground substance: 23%
- Blood vessels: 60%
- Connective tissue: 7%
- Collagen: 4%
- Empty space: 6%

1. Frank J, Langer G. J Cell Biol 1974;60:586-901.

Figures: (Left) Rutherford SL et al. Circ Res 2012;111:301-11
(Right) Plank G et al. Phyl Trans R Soc A 2009;367:2257-92

Inter-subject anatomical variability in Purkinje system

Bordas et al. IEEE EMBC, 2010

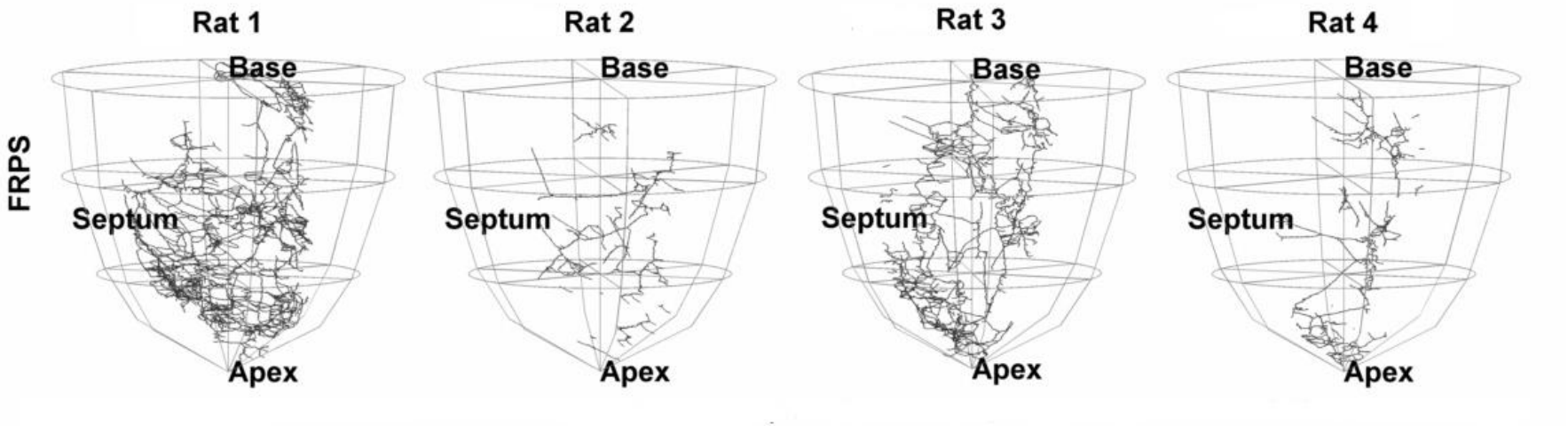

Hypertrophic cardiomyopathy: myocyte disarray and fibrosis

Inherited Cardiomyopathies, New England J. of Medicine, H.Watkins et al., 2011

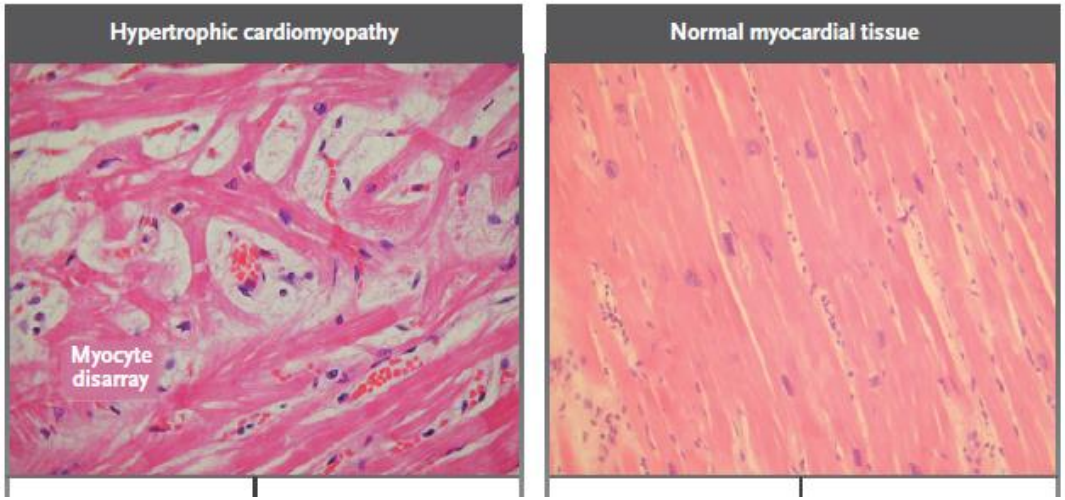

Multiscale Mechanisms from ion channels to ECG

Tissue/Organ (Optical mapping, MRI)

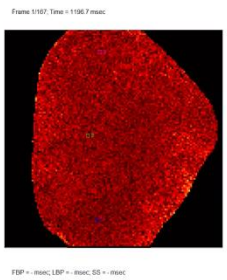

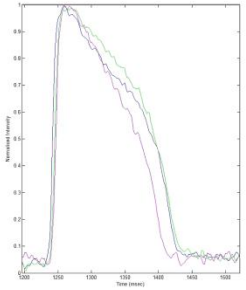

Propagation model

$$\nabla \cdot \bar{\sigma}_i \nabla \Phi_i = \beta \cdot I_m - I_{st\_i}$$

$$\nabla \cdot \bar{\sigma}_e \nabla \Phi_e = -\beta \cdot I_m$$

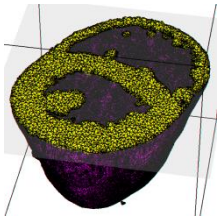

Cell (Microelectrode)

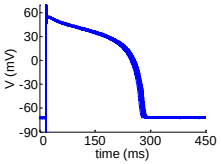

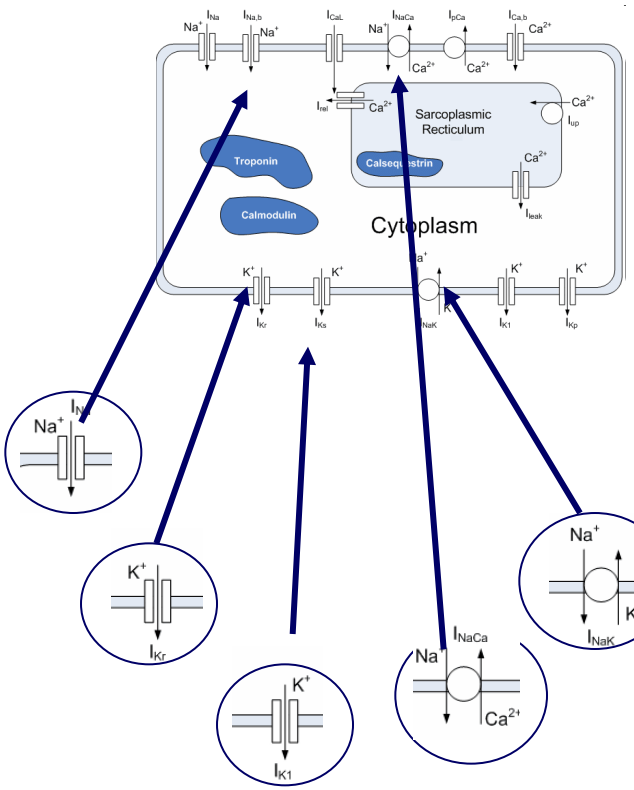

Action potential model

$$I_{stim} = C\frac{dV_m}{dt} + I_m$$

Ionic current (Voltage-clamp)

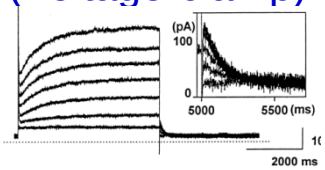

Ionic current models

$$I_{Na} = g_{Namax} * m^3 * h * j * (V_m - E_{Na})$$

$$\frac{dx}{dt} = \alpha_x(1-x) - \beta_x x$$

$$\alpha_x = \alpha_x(V_m); \beta_x = \beta_x(V_m)$$

Spatial heterogeneity and fractional models

Mathematical modelling of cardiac tissue

- The traditional way of modelling wavefront propagation in the heart is to represent the **tissue as a continuum** with spaced averaged properties:

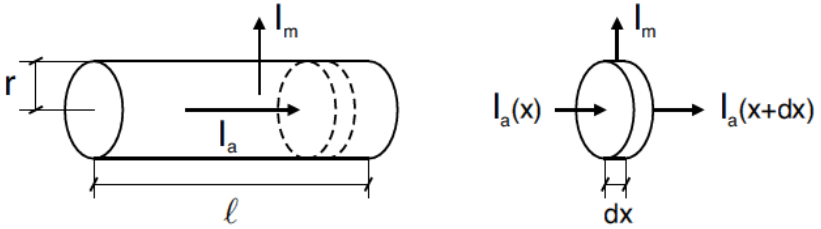

$$\partial_t V_m = -D\nabla\left(-\nabla V_m\right) - \frac{1}{C_m} I_{\text{ion}},$$

I_{ion} : ODE system describing cell dynamics (electrophysiology)

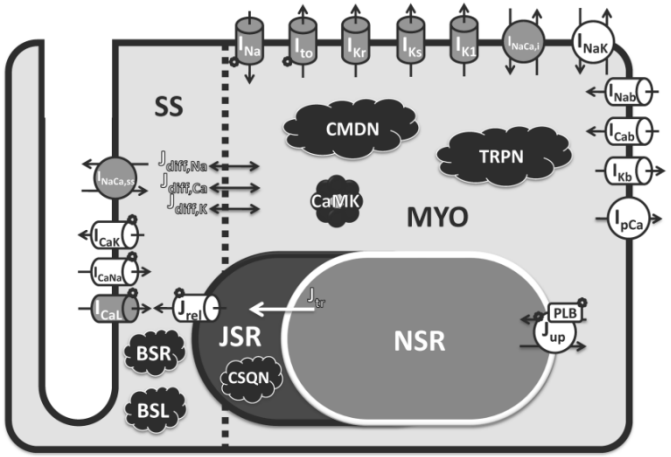

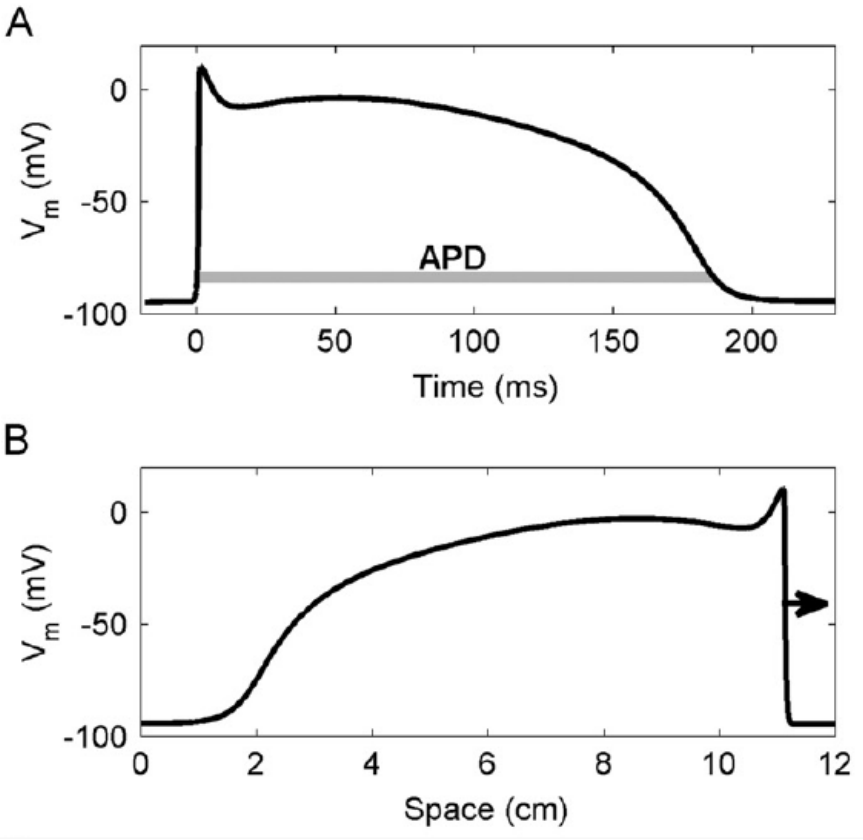

Figures: (Left) O'Hara T et al. PLoS Comput Biol 2011;7:e1002061
(Right) Cherry EM, Fenton FH. J Theor Biol 2011;285:164-76

Fractional diffusion as a tool to describe heterogeneous media

- Many systems characterised by structural heterogeneity, where transport is facilitated within a certain scale, exhibit **heavy-tailed experimental distributions** (filtration of solutes in porous soils, diffusion of colloids in polymers, MRI, ...).

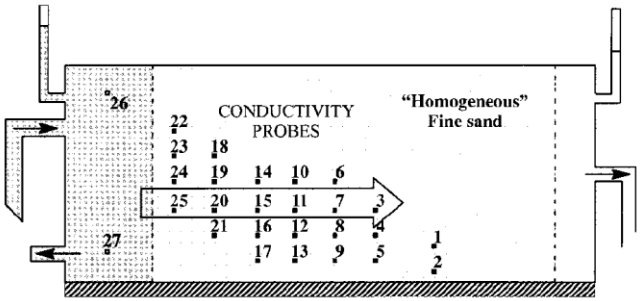

Benson DA et al. Water Resour Res 2000;36:1403-12

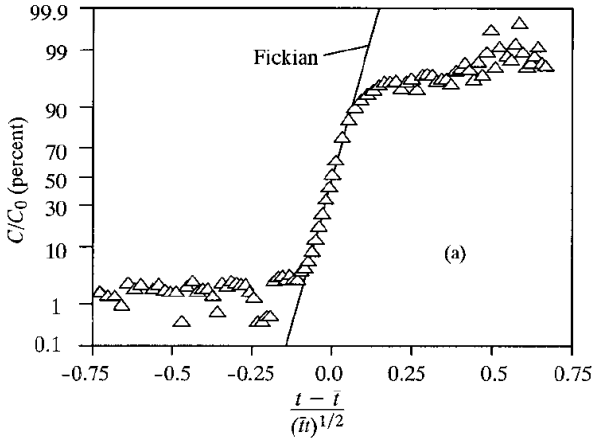

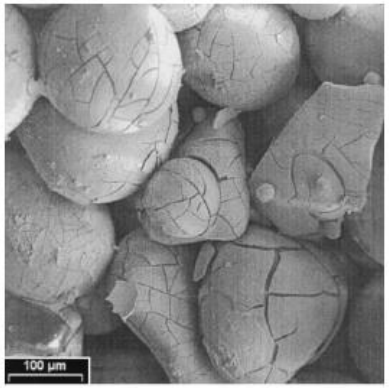

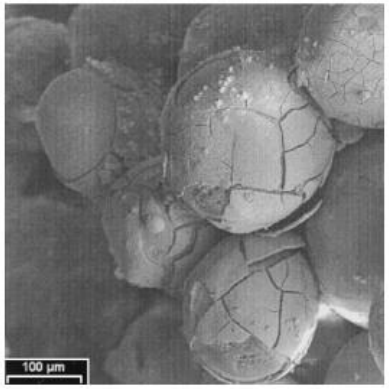

- Many authors have shown the equivalence between heavy-tailed motions and transport equations that use **fractional-order (non-integer) derivatives.**

- These models can be rigorously derived from an ensemble of particles undergoing **stochastic Levy walks,** with more heavy-tailed probabilistic distributions as the fractional order separates from the integer (standard) derivative.

Fractional monodomain equation

- A fractional monodomain equation can be considered by replacing the current flux through the membrane to the heterogeneous extracellular domain by its fractional counterpart:

$$\partial_t V_m = -D\nabla^\beta(-\nabla V_m) - \frac{1}{C_m} I_{\text{ion}}, \quad 0 < \beta \leq 1,$$

where ∇^β is the Riemann-Liouville fractional gradient:

$$\frac{\partial^\beta}{\partial x^\beta} u(x,y,z) = \frac{1}{\Gamma(1-\beta)} \frac{\partial}{\partial x} \int_0^x \frac{u(s,y,z)}{(x-s)^\beta}\, ds,$$

- Alternatively, in the isotropic setting we can rewrite by considering the use of Riesz potential theory:

$$\partial_t V_m = -D_\alpha(-\Delta)^{\alpha/2} V_m - \frac{1}{C_m} I_{\text{ion}}, \quad 1 < \alpha \leq 2$$

- **Q:** Can we recover important phenomena of cardiac tissue by considering this **fractional diffusion formulation of wavefront propagation?!?**

Biophysical justification of fractional diffusion: Potential Theory

- Fractional diffusion model of excitable tissue:

$$\partial_t V_m = -D\nabla\left(-\nabla V_m\right) - \frac{1}{C_m} I_{\text{ion}}, \rightarrow \partial_t V_m = -D_\alpha(-\Delta)^{\alpha/2} V_m - \frac{1}{C_m} I_{\text{ion}}, \quad 1 < \alpha \leq 2$$

- Only coupling is modified → let's analyse solutions of: $-\Delta\phi = \frac{I}{\sigma}$ (N=3 dimensions)

- **Homogeneous tissue**, $I = I_0\delta(r)$:

$$\phi_m(r) = \frac{I_0}{4\pi\sigma r} \quad \rightarrow \quad \phi(r) \sim 1/r$$

- **Tissue inhomogeneities**[1]:

$$\phi_p(r) = \frac{1}{4\pi\sigma_p} \sum_i \oint_{S_i} \delta\sigma_i \cdot \phi_i \frac{\vec{a}_r \cdot d\vec{S}}{r^2}$$

$$\rightarrow \quad \phi(r) \sim 1/r^2$$

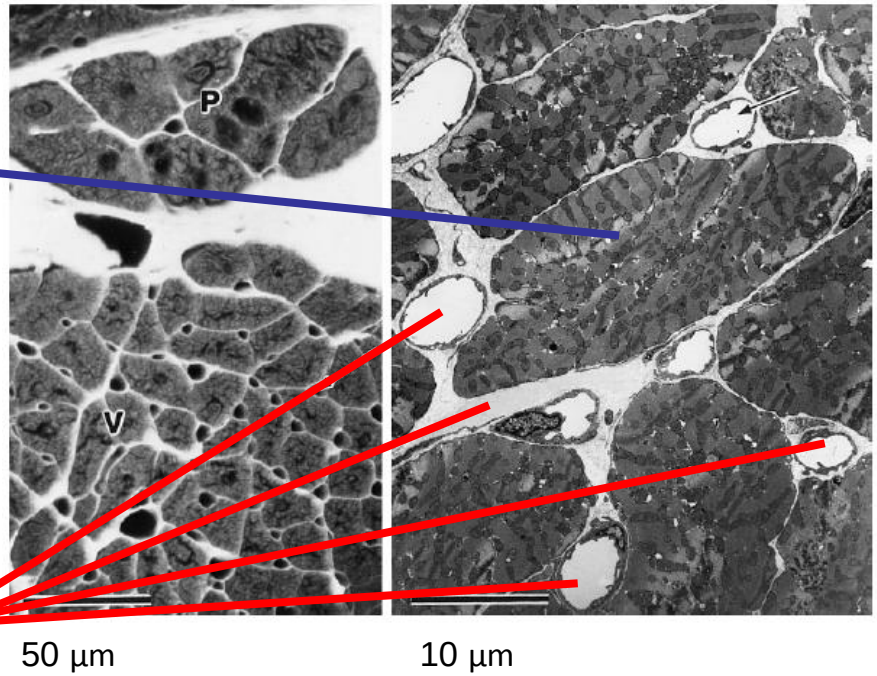

1. Plonsey R. & Barr R. "Bioelectricity: A quantitative approach", Springer, 2007.

Figure: Spach MS et al. Circ Res 1998;93:1144-64.

Biophysical justification of fractional diffusion: Potential Theory

- Riesz potential of the fractional Laplacian:

$$(-\Delta)^{\alpha/2}\phi = C_\alpha \int_{\mathbb{R}^N} \frac{\phi(r)-\phi(r')}{\|r-r'\|^{N+\alpha}}\,dr' \qquad C_\alpha = \frac{\pi^{N/2}\,2^\alpha\,\Gamma(\frac{\alpha}{2})}{\Gamma\left(\frac{N-\alpha}{2}\right)}$$

- Therefore, the potential associated to the fractional Laplacian is:

$$\phi(r) = (-\Delta)^{-\alpha/2} f = \frac{1}{C_\alpha} \int_{\mathbb{R}^N} \frac{f(r')}{\|r-r'\|^{N-\alpha}}\,dr'$$

- **α = 2** ($N = 3$ and $f = I_0\delta(r)/\sigma,$) :

  $\phi(r) \sim 1/r$ → homogeneous tissue

- **α = 1** ($N = 3$ and $f = I_0\delta(r)/\sigma,$) :

  $\phi(r) \sim 1/r^2$ → tissue inhomogeneities

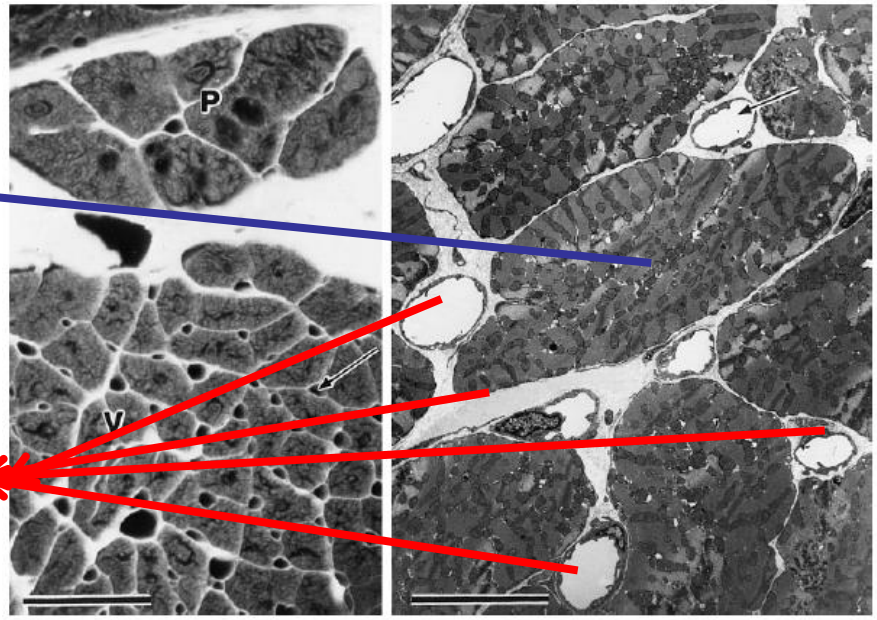

50 µm 10 µm

Figure: Spach MS et al. Circ Res 1998;93:1144-64.

Numerics and getting the boundary conditions right in fractional models

Fisher Equation

Standard steady speed travelling wave

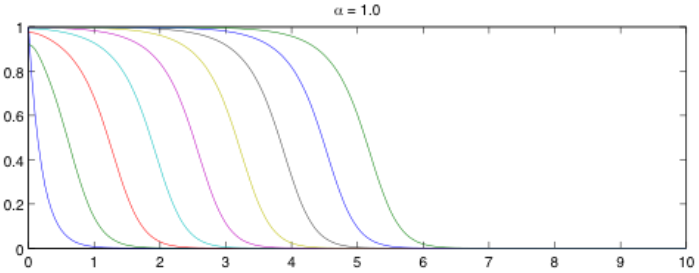

$$\frac{\partial u}{\partial t} + \nu(-\Delta)^{\alpha} u = u(1-u) \qquad \text{in } \Omega,$$

$$\frac{\partial u}{\partial n} = 0 \qquad \text{on } \partial\Omega,$$

$$u(x,0) = u_0(x) \qquad \forall x \text{ in } \Omega.$$

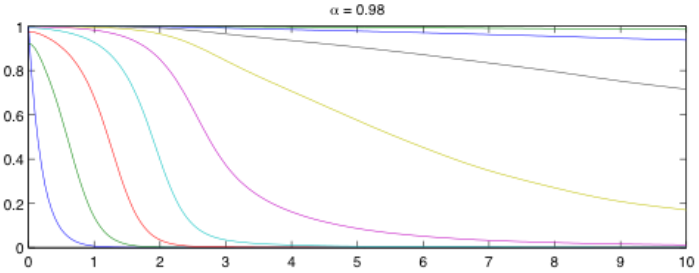

Exponential spread of the interface is clearly seen, see Engler 2010.

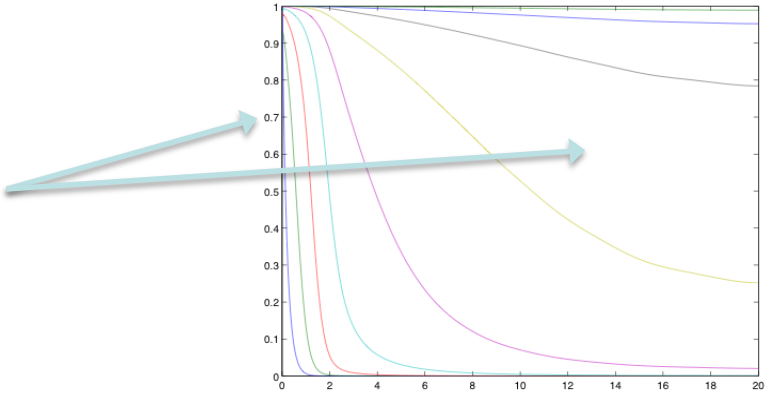

Reflecting Boundary Conditions

Using the Generalised Master Equation (GME) we can derive a space-fractional equation involving the Riesz-Feller operator for the probability density function of an ensemble of particles undergoing a Levy walk CTRW.

By introducing reflecting boundaries, a jump from x1 to x2 both in the finite domain [0; L], may be obtained in an infinite number of ways via repeated bounces from the walls x = 0 and x = L.

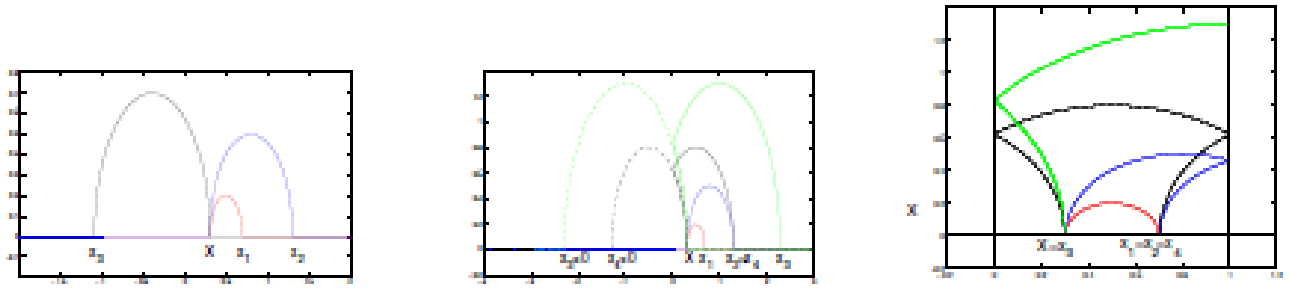

(a) Infinite domain (b) Semi–infinite domain (c) Bounded domain

FIG. 2.1. *Transitions of an ensemble of particles based on α-stable symmetric Lévy walks on infinite, semi–infinite and bounded domains.*

REFLECTIONS FROM A BOUNDARY: REFLECTING BOUNDARY CONDITIONS FOR SPACE-FRACTIONAL PARTIAL DIFFERENTIAL EQUATIONS ON BOUNDED DOMAINS

DAVID KAY†, IAN TURNER‡, NICOLE CUSIMANO‡ AND KEVIN BURRAGE§

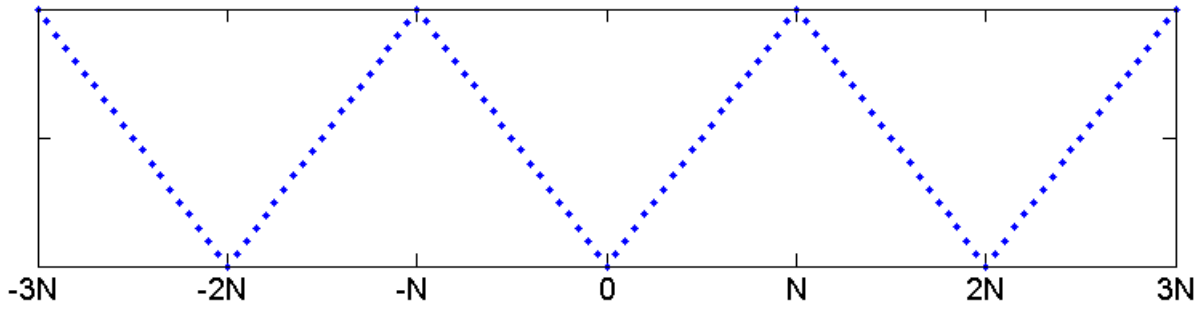

Let $k_{\max}$ be the number of teeth of the sawtooth function considered in the approximation and $j_{\max} = 2Nk_{\max}$, then at each node of the spatial mesh we obtain the following discretization:

$$u_i^{n+1} + \frac{\Delta t\ c^\alpha}{h_x^\alpha}\left[\sum_{j=-1}^{j_{\max}} \omega_j^\alpha \left(u_{[i-j]_0^N}^{n+1} + u_{[i+j]_0^N}^{n+1}\right)\right] = u_i^n.$$

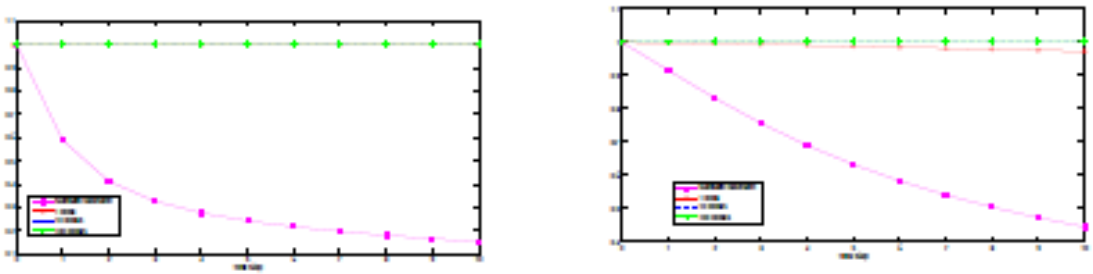

(a) $\beta = 0.9$ (b) $\beta = 0.05$

FIG. 3.1. *Total mass is not conserved with standard Neumann boundary conditions (pink), but with the correct reflecting boundary conditions, mass is increasingly conserved as the number of reflective blocks increase. Here $\beta = 0.9$ and $\beta = 0.05$, the initial condition is $P(0, x) = \delta(x - 0.05)$ and the number of blocks is 1, 10, 100 (green).*

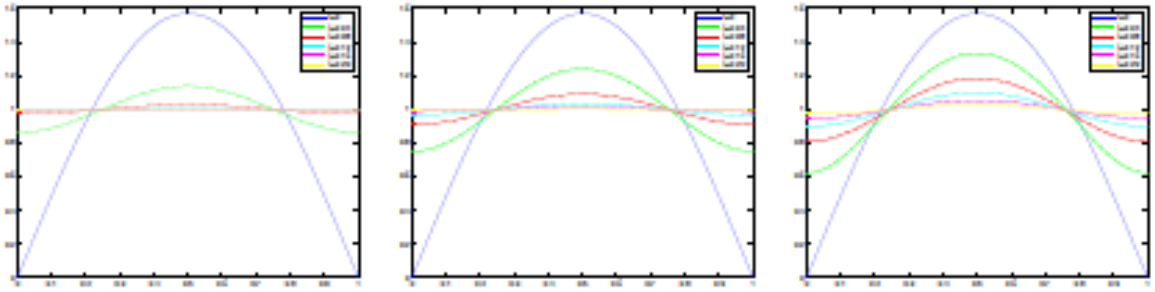

(a) $\alpha = 2.0$ (b) $\alpha = 1.75$ (c) $\alpha = 1.5$

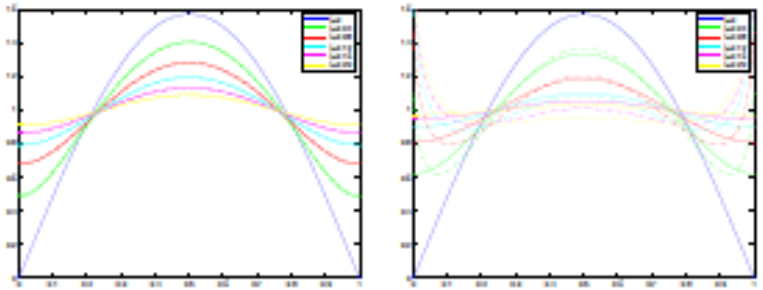

(d) $\alpha = 1.25$ (e) $\alpha = 1.5$ with standard Neumann BCs

FIG. 4.1. *Simulations with the new reflecting boundary conditions at both* $x = 0$ *and* $x = 1$, *initial condition* $u_0(x) = \frac{\pi}{2} sin(\pi x)$, *(a)-(d). Figure (e) shows the behaviour under standard Neumann boundary conditions*

Validation of a fractional monodomain model

$$\partial_t V_m = -D_\alpha(-\Delta)^{\alpha/2} V_m - \frac{1}{C_m}(I_{\text{ion}} - I_{\text{stim}}), \quad 1 < \alpha \leq 2,$$

$$\partial_t \mathbf{y} = \mathbf{f}(V_m, \mathbf{y}), \quad I_{\text{ion}} = \mathbf{g}(V_m, \mathbf{y})$$

Neonatal rat cell cultures (“the heart in a dish”)

- *N.Badie &N. Bursac, Novel Micropatterned Cardiac Cell Cultures with Realistic Ventricular Microstructure, Biophysical J. Vol. 96 May 2009 3873–3885.*

•Systematic studies of cardiac structure-function relationships is hindered by the intrinsic complexity and variability of in vivo and ex vivo model systems.

•The authors develop a reproducible cell culture system that can replicate the realistic microstructure of native cardiac tissues using cell micropatterned cardiac cultures with realistic tissue boundaries and natural cell orientation, random cell orientation, and standard isotropic monolayers.

• They aligned cultured cardiomyocytes at micro- and macroscopic spatial scales to follow local directions of cardiac fibres in murine ventricular cross sections, as measured by high-resolution diffusion tensor magnetic resonance imaging.

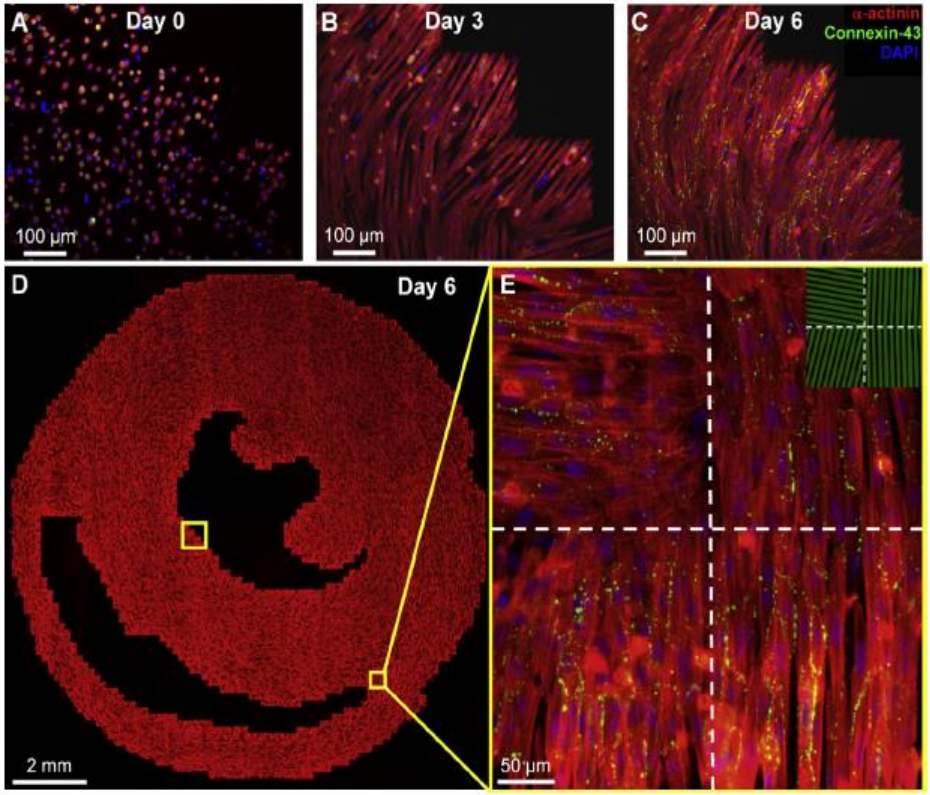

FIGURE 3 Formation of realistic cardiac microstructure in AS cultures. (*A–C*) Plated cells were found to attach (*A*), spread and align along the underlying fibronectin lines (*B*), and by day 6 (*C*) form confluent cardiac fibers. (*D*) Composite image of the entire micropatterned slice culture. (*E*) Close-up of four adjacent pixels delineated by dashed lines, along with the underlying fibronectin pattern (*green, inset*). Note abrupt changes in cardiac fiber directions in neighboring pixels without loss of cell confluence.

Neonatal rat cell cultures (“the heart in a dish”)

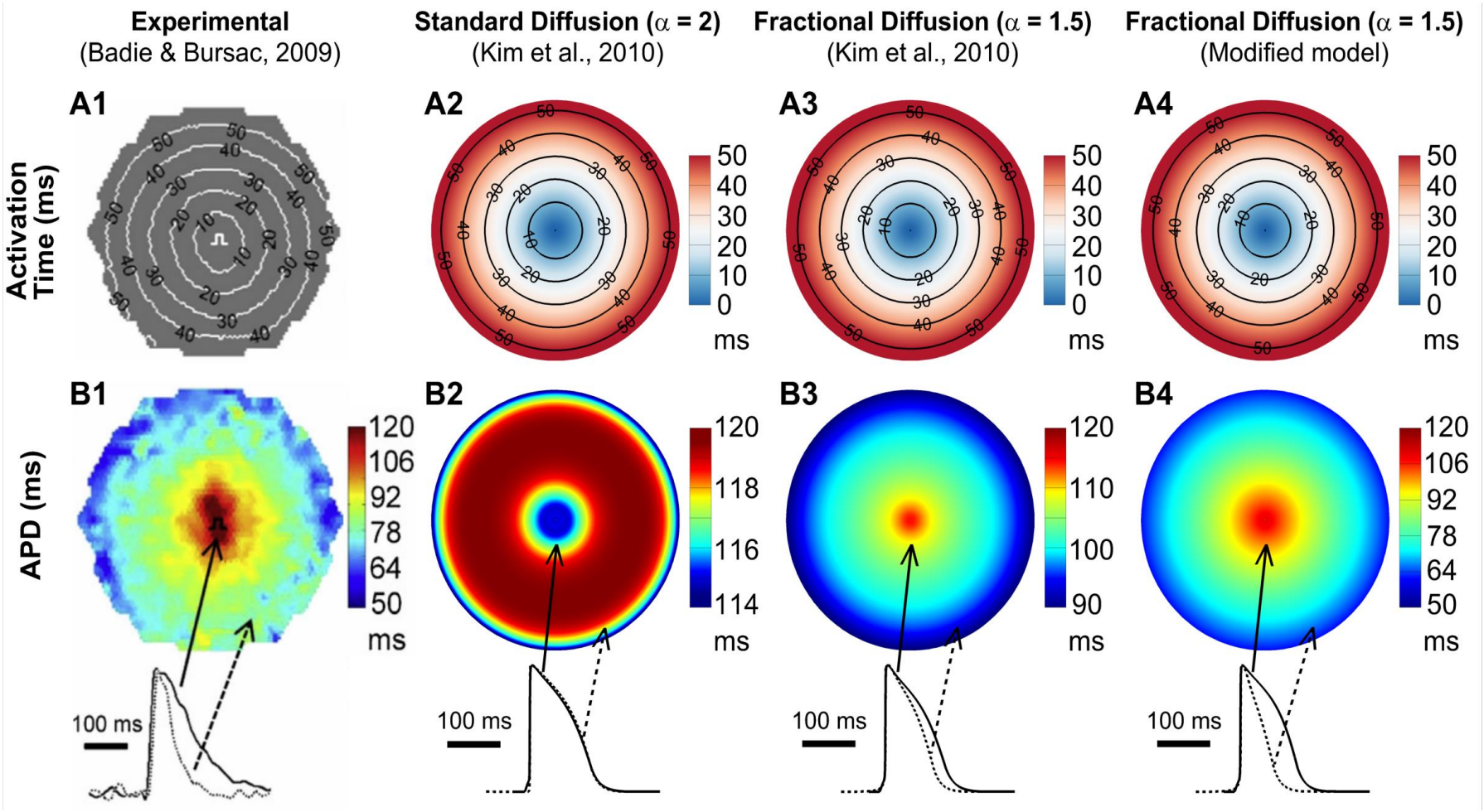

Fractional diffusion models of electrical propagation in cardiac tissue: nonlocal electrotonic effects modulate cellular repolarization, submitted to Nature Comms, 2013, A. Bueno-Orovio, D. Kay, V. Grau, B. Rodriguez, K. Burrage.

The inverse AT-APD relationship

- A compelling mechanism of the intact heart is the **shortening of APD along the activation path** (a.k.a. the inverse Activation time (AT)-APD relationship).

- It has been **reported in multiple studies and different species** (including in-vivo human, in-vivo dog, or isolated rabbit and guinea pig hearts).

- Furthermore, it is considered a **natural cardioprotective mechanism of the intact heart,** since it contributes to reduce total dispersion of repolarization.

- In fact, AT-APD relationships have been shown to be less steep in diseased hearts[1].

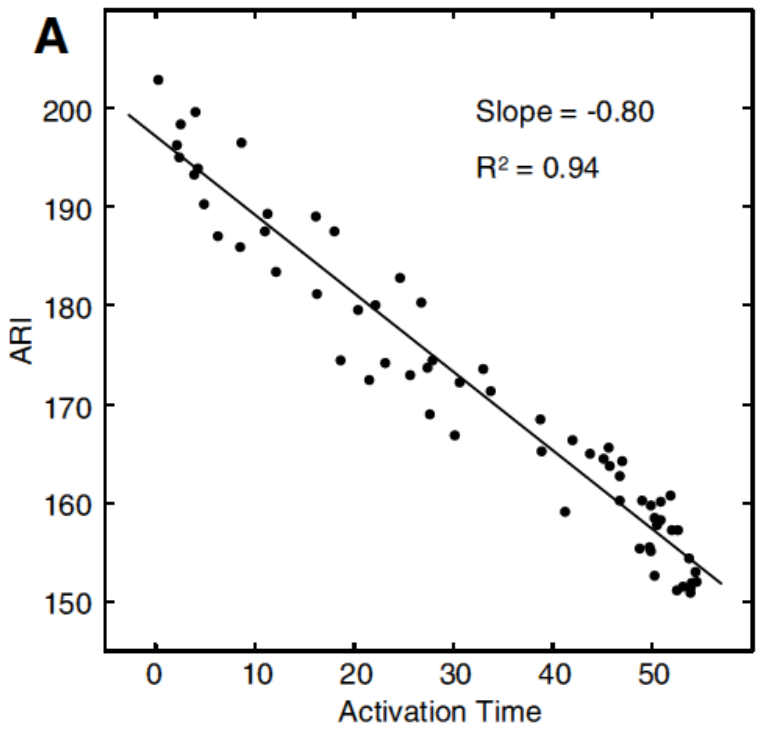

Experimental data:
Hanson B et al. Circ Arrythmia Electrophysiol 2009;2:162-70

1. Cowan JC et al. Br Heart J 1998;60:424-433.

The inverse AT-APD relationship: electrotonic effects

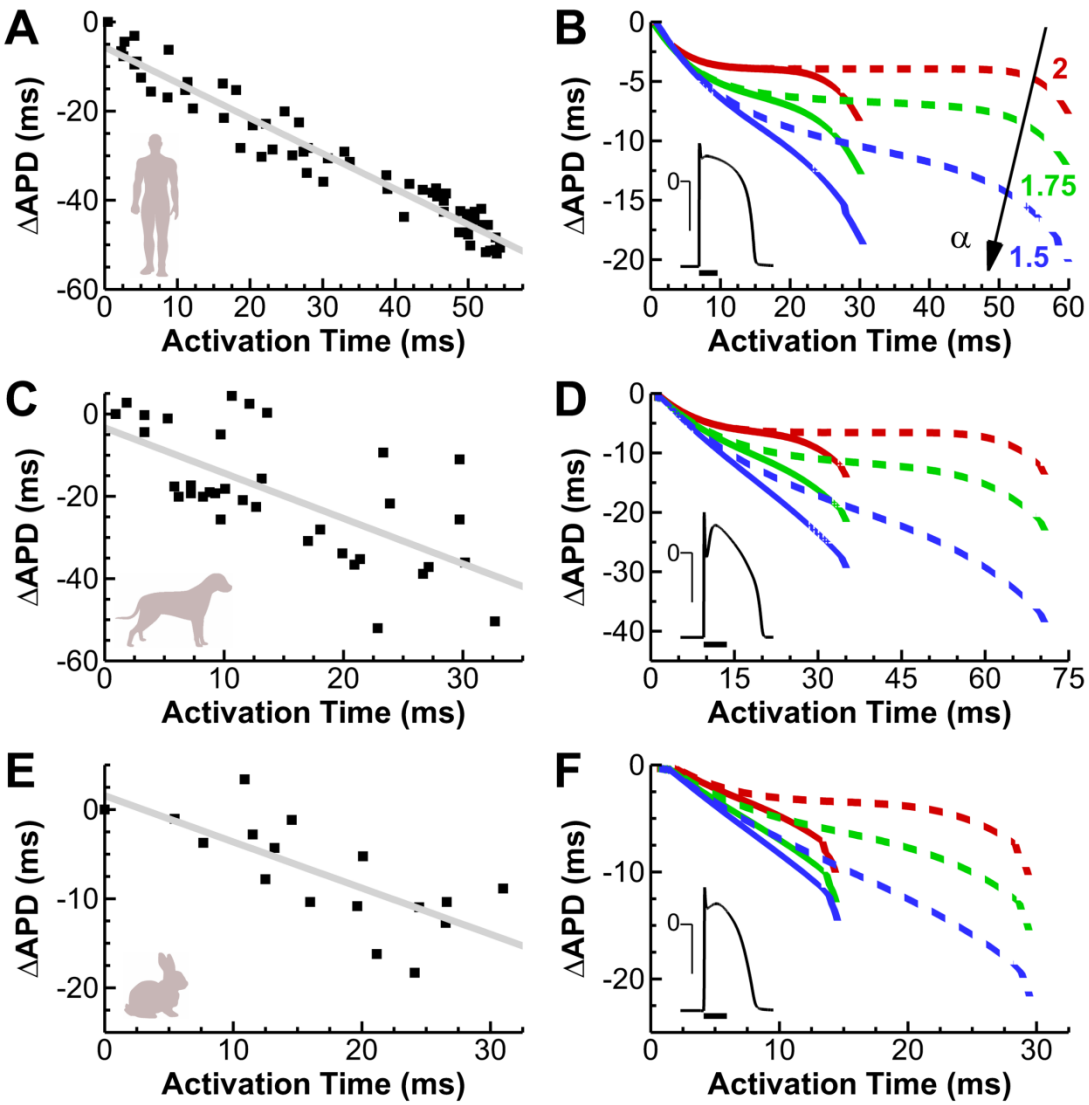

Shortening of APD during propagation.
1D cable solid 2cm, dash 4.
Standard diffusion has moderate dispersion regardless of cell type.
Change in APD increasingly large for decreasing alpha.

Tissue dispersion of APD restitution

Experimental data:
Hanson B et al. Circ Arrythmia Electrophysiol 2009;2:162-70

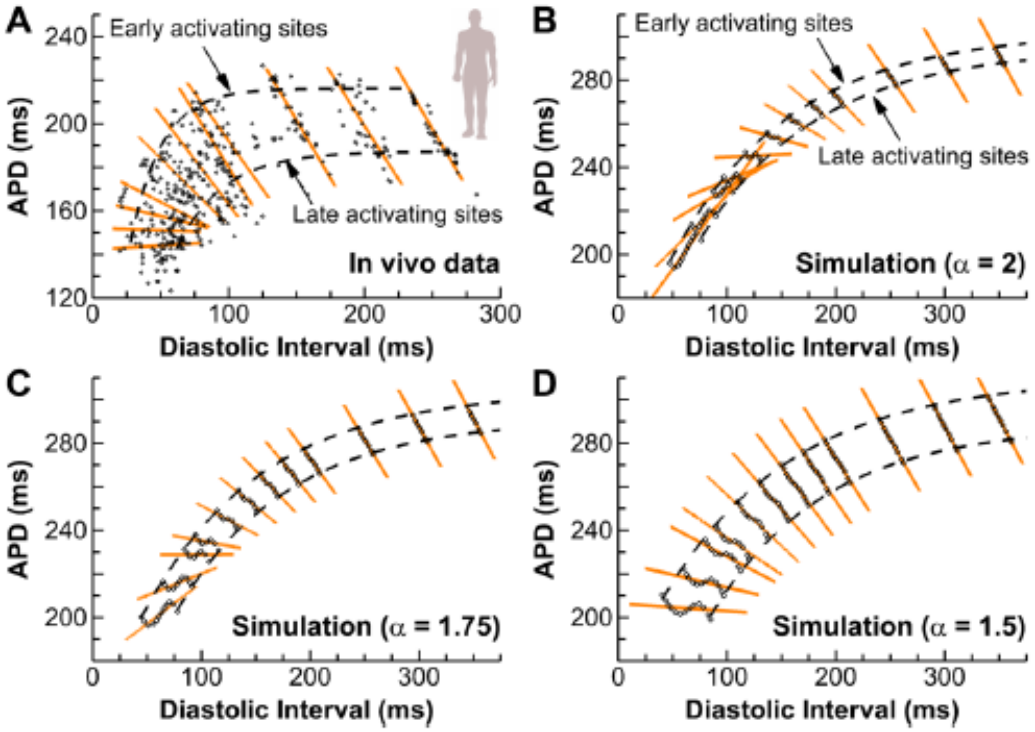

A: Experimental data from multiple sites from healthy human endocardium. Linear regression lines are shown for APD versus DI at each test coupling interval, exhibiting a progressive flattening of slope as the coupling interval shortens.
B: Global DI-APD dependence in a simulated cable of human cardiac tissue of 4 cm length (alpha=2). Dispersion between early and late APD restitution curves small, but regression lines manifest a rapid inversion of slopes at short coupling intervals.
C, D: Global DI-APD dependence for fractional diffusion models (alpha=1.75 and 1.5). The separation between early and late APD restitution curves increases for decreasing fractional order, also recovering the progressive flattening of regression lines.

Discussion

Issues with fractional models and application to the heart

•Two principal hypotheses employed by standard theories of diffusion are that the continuum hypothesis uses local averaged values and the Fickian law for the flux is defined in terms of the gradient of the quantity involved.

•The averaged quantity fluctuates as the averaging volume becomes smaller and homogenisation can fail in heterogeneous settings. But bidomain theory has been very successful since 1975.

•The non-homogeneities of the medium alter the laws of Markov diffusion - heavier tail than the Gaussian density, resulting in long-range dependence.
This is related to Levy flights – but what are they biophysically?

• Should we just view fractional models as phenomenological?

• However, Riesz potential is a generalisation of standard potential theory based on the inverse of a fractional Laplacian.

• Inhomogeneities lead to generation of secondary dipoles. We can modify standard monopole theory for electrical propagation and use the idea of fractional conductance – first proposed in semi-conductor theory.

$$I(r) = (r^{\alpha-1}/4\pi r^2)(I_0/\sigma)$$

Philosophical musings

- What do we want from a model?
  - What are the questions? What data do we have?
- Should we add increasing complexity just because we can?
- Should a model be intuitive?
- The roles and use of phenomenological models versus biophysically detailed models at the Cell level or Tissue level.
- How do we validate a fractional model? Diffusion Tensor MRI. Need a fractional Bloch-Torrey model to build a model and fit data.
- What level of complexity should a fractional bidomain model have? Is this a mechanism for APD dispersion?
- Can we use fractional bidomain models for patient specific heart data?

- A. Carusi, K. Burrage, B. Rodriguez (2012): Bridging Experiments, Models and Simulations: An Integrative Approach to Validation in Computational Cardiac Electrophysiology, Am. J. Physiology.
- *Phenomenological modeling of cell to cell-to-cell and beat-to-beat variability in isolated guinea pig ventricular myocytes, J. Walmsley, G. Mirams, M. Bahoshy, C. Bollensdorff, B. Rodriguez and K. Burrage, 2010 .*
- *A practical implementation of an implicit FEM scheme for equations with fractional diffusion. K. Burrage, N. Hale and D. Kay, SISC, 34, 2145-2172, 2012.*

Acknowledgements:

Australia (QUT)
P. Burrage, F.Liu, I.Turner.
T. Moroney, Q. Yang.

Oxford
Blanca Rodriguez, Annamaria Carusi, Ciara Dangerfield, Vicente Grau, Nick Hale, David Kay, Alfonso Bueno-Orovio, John Walmsley.

Spain
Esther Pueyo (Zaragoza)